

Diffusion of water vapour in cellulose acetate:

1. Differential transient sorption kinetics and equilibria

P. P. Roussis

Physical Chemistry Laboratory, Demokritos Nuclear Research Center, Aghia Paraskevi, Attiki, Greece

(Received 11 April 1980; revised 30 June 1980)

The concentration dependence of the diffusion coefficient D , of the cellulose acetate/water vapour system has been investigated: aspects of the non-Fickian behaviour of the system are reported. Kinetic and equilibrium data, were obtained for membranes of different thicknesses from a series of differential sorption experiments along both limbs of the hysteresis loop. The data are treated in alternative ways. It is concluded that we may distinguish two rate-determining molecular relaxation processes: a relatively fast one, prevailing during the initial stages of absorption, which is succeeded by a considerably slower and more drastic reorganization of the polymer structure. During the latter stage the solubility coefficient S is shown to possess a long-term time dependence, which is attributed to penetrant cluster formation. D obtained from desorption kinetics increases with concentration, whereas the apparently concentration-independent D on the absorption side is assumed to be due to partial immobilization of penetrant in regions where penetrant clusters are developed.

INTRODUCTION

The importance of the cellulose acetate-water system in several industrial fields, particularly reverse osmosis, has resulted in the attention of investigators¹⁻¹⁰. These studies involve vapour permeability measurements by the 'cup' method or by use of more sophisticated equipment; alternatively equilibrium and transient-state sorption data within the range $0 \leq a \leq 1$ of penetrant vapour activity a . For a given activity, a wide spread of values of the diffusion coefficients D (of the order of $1.5-4.0 \times 10^{-8} \text{ cm}^2 \text{ s}^{-1}$) is reported. Comparison of these data also reveals certain contradictions concerning the dependence of D on a (or on the corresponding vapour concentration C in the polymer); in most cases D is shown either to be constant^{6,7}, or slightly increasing with C , with a tendency for a steeper increase close to saturation⁹, but D has also been reported to decrease with C ¹⁰. Another important ambiguity to be resolved is the contradictory conclusions which may be drawn concerning the nature of the 'non-Fickian' behaviour of this system upon analysis of published results on sorption and permeation¹¹. Several experimental factors are involved in these studies (e.g. acetyl content, membrane fabrication procedures, experimental conditions, method of measurement and data treatment). The existence of sorption hysteresis constitutes an additional complication. It is thus difficult to separate these from purely intrinsic effects in order to account fully for the discrepancies and disagreements.

Taking all these factors into consideration, this investigation aimed to elucidate some of the anomalies by performing a series of differential absorption and corresponding desorption kinetic experiments along the two limbs of the hysteresis loop. In an attempt to distinguish diffusion from other rate-determining processes, data on

four membranes of different thicknesses are analysed. Supplementary results on long-term permeation and integral sorption are compared in a subsequent paper.

THEORETICAL

Consider that the unidimensional diffusion axis, X , lies across a membrane of thickness l . The boundary conditions within the region $0 \leq X \leq l$ may be defined in terms of the following vapour activities, which at any time $t \geq 0$ of an experiment are maintained constant:

$$a(X=0, t) = a_0; a(X=l, t) = a_l; a(X, t=0) = a_1 \quad (1)$$

In sorption kinetics $a_0 = a_l$ ($a_0 > a_1$ in absorption and $a_1 < a_0$ in desorption). The term 'differential sorption' signifies a series of n experiments for which a_1 (for the i th run) $= a_0$ (for run $i-1$). The measurable quantity is Q_t , the amount sorbed per unit membrane area, and from its equilibrium value Q_∞ (at $t \rightarrow \infty$) the solubility coefficient $S = C/a$ is determined. A prerequisite for normal 'Fickian' diffusion is that equilibria between the penetrant and the membrane at any X are attained instantaneously, so that the constants in equations (1) can also be expressed in terms of the corresponding concentrations $C_0 = Sa_0$, $C_l = Sa_l$, $C_1 = Sa_1$ and diffusion is described by:

$$\frac{\partial C}{\partial t} = \frac{\partial}{\partial X} \left[D \frac{\partial C}{\partial X} \right] \quad (2)$$

Another condition for Fickian diffusion is that D is either constant or merely concentration dependent. For constant D , equation (2) affords analytical solutions which can be approximated by the following expressions¹²:

Table 1 Experimental conditions for the second increment in absorption kinetics

Membrane	l (μm)	a_1	a_0	C_1 (g/g)	C_0 (g/g)
1	186	0.184	0.354	0.0152	0.0312
2	267	0.192	0.359	0.0165	0.0301
3	366	0.181	0.348	0.0149	0.0280
4	99	0.185	0.356	0.0166	0.0300

$$\frac{Q_t}{Q_\infty} = 4 \left[\frac{D_1 t}{\pi l^2} \right]^{1/2} \quad (3)$$

$$\ln(1 - Q_t/Q_\infty) = \ln \left[\frac{8}{\pi^2} \right] - \frac{D_2 \pi^2 t}{l^2} \quad (4)$$

Equations (3) and (4) are pertinent to early and long times, respectively, and can be used even for concentration-dependent systems to obtain the differential diffusion coefficients D_1 and D_2 provided that the concentration interval $C_0 - C_1$ is sufficiently small.

However, sorption in polymer-vapour mixtures below the glass transition temperature is known to depart from the patterns described by equations (3) and (4) in a variety of ways¹¹ (some of which are illustrated later). In terms of the molecular relaxation model^{13,14} these discrepancies are due to the relatively slow rate of rearrangements in the polymer structure, which are necessary to accommodate the penetrant molecules. Earlier versions of this model assumed either D or C_0 (Crank¹³ and Long and Richman¹⁴, respectively) approached their equilibrium values $D(a, \infty)$ or $C(a, \infty)$ according to a first order kinetic parameter β (which is the relaxation frequency in s^{-1}), when the magnitude of the βl^2 is comparable to that of D . As a result, either of the aforementioned conditions for normal Fickian diffusion is violated.

An alternative or unified version of the above models^{11,15-17} considers the 'thermodynamic' permeability P_T as well as S to be time-dependent coefficients and employs the following formulation instead of equation (2):

$$\frac{\partial C}{\partial t} = \frac{\partial}{\partial X} \left[D_T S \frac{\partial a}{\partial X} \right] = \frac{\partial}{\partial X} \left[P_T \frac{\partial a}{\partial X} \right] \quad (5)$$

where D_T is the 'thermodynamic' diffusion coefficient, which is a direct measure of penetrant mobility. Thus, depending on the way D_T and S vary with t , the equilibrium value of the permeability $P_T(a, \infty)$ is approached from an initial $P_T(a, 0)$ according to a rate constant β . This model virtually accepts that the already documented¹⁴ gradual increase in the surface concentration C_0 is simply evidence that the sorptive capacity of the entire membrane is time variable, so that the rate of change in $C(a, t)$ in the absence of a concentration gradient may be expressed in the following general way:

$$\frac{\partial C}{\partial t} = \frac{\partial C(a, 0)}{\partial a} \frac{\partial a}{\partial t} + \beta \{C(a, \infty) - C(a, t)\} \quad (6)$$

If equations (5) and (6) are solved simultaneously, sorption kinetic curves are obtained for a set of assumed conditions which resemble experimental results reported in the literature^{11,16}.

EXPERIMENTAL

Cellulose acetate was in the form of filtered powder (kindly supplied by Eastman Chemicals, type E-400-25, 39.9% acetyl content, density 1.30 g cm^{-3}). Four membranes (see Table 1) were prepared by casting 20% acetone solutions of the polymer on clean glass surfaces; their thicknesses (determined by weight and area measurements) are given in Table 1. The solvent was removed by slow evaporation and its final traces were leached out by conditioning the films in water at 65°C for several hours. Prior to each sequence of experiments the membrane was completely evacuated, equilibrated at $a = 1$ and finally re-evacuated.

During a run, a_0 was maintained constant by controlling the vapour generator at the appropriate temperature to $\pm 0.02^\circ\text{C}$. The membrane was suspended from pre-calibrated quartz springs (sensitivity 25 cm g^{-1}) inside the sorption chamber, which was thermostatically controlled at $25^\circ \pm 0.05^\circ\text{C}$ by circulating water from a constant temperature bath to a surrounding glass jacket. The rate of sorption was monitored by measuring the elongation of the quartz springs by means of a precision cathetometer, which was also used for vapour pressure readings on a closed-end mercury manometer.

RESULTS

For reasons of comparison under similar experimental conditions, each differential sorption run was performed at approximately the same a_1 and a_0 on all membranes, as shown in Table 1 for one such increment. Figure 1 shows the distinct hysteresis effect observed in the isotherm of this system; it was drawn after fitting the experimental equilibrium points (of seven successive increments along either limb of the hysteresis loop) to a fifth degree polynomial. Equilibrium points were recorded when the quartz spring elongation remained constant for at least 24 h. The double arrows in Figure 1 represent the spread of experimental data, which becomes significant at higher concentrations, especially on the desorption side of the isotherm.

The kinetic data for the family of sorption runs in Table 1 (Figure 2a) show the characteristics of non-Fickian

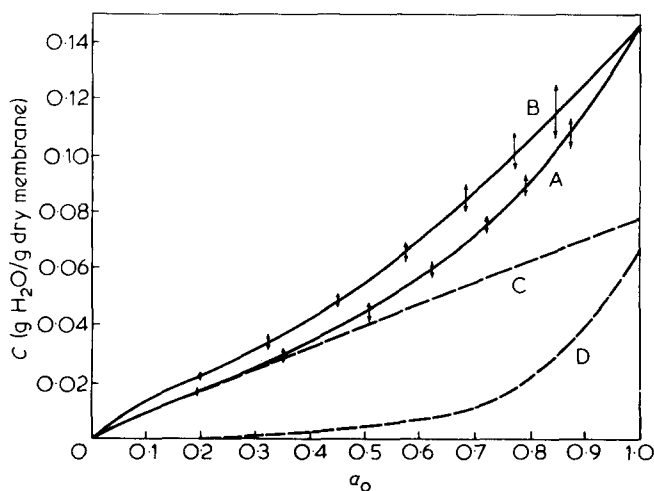


Figure 1 Sorption isotherm at 25°C . Curves: A, absorption; B, desorption; C, C_m in absorption (calculated); D, C_a in absorption (calculated)

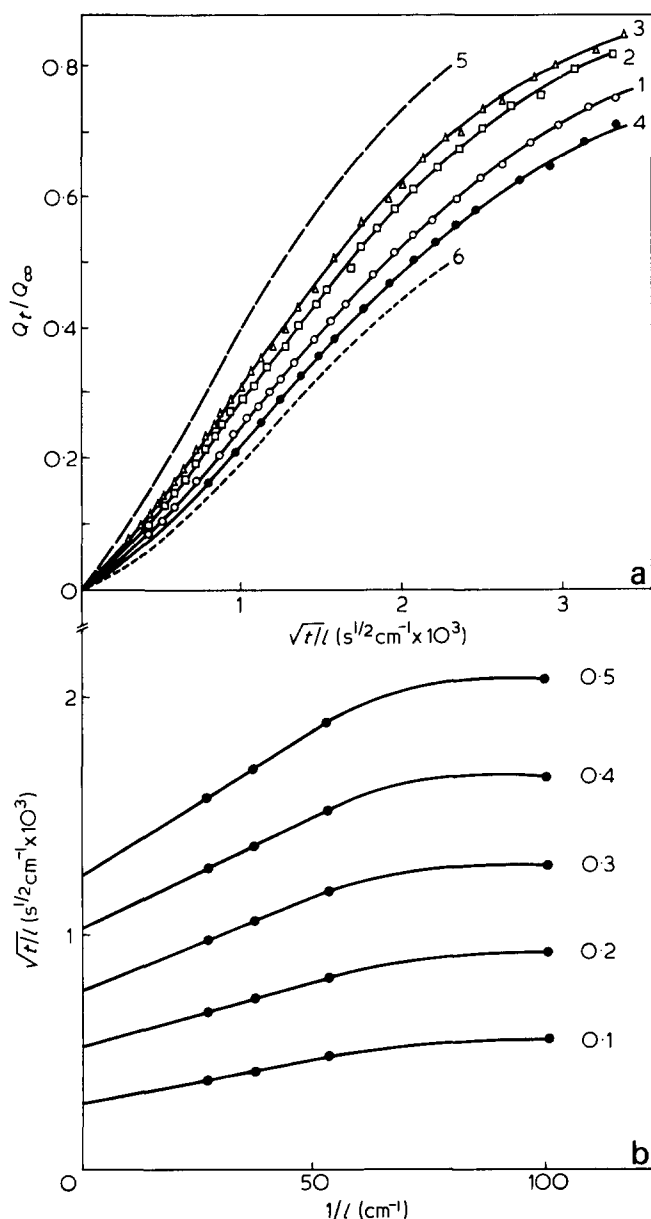


Figure 2 (a) Differential absorption kinetics on membranes 1–4 and conditions given in Table 1; curve 5, $l \rightarrow \infty$ (extrapolated); curve 6; $l \rightarrow 0$ (extrapolated). (b) Extrapolation to $l \rightarrow \infty$ for curves of Figure 2a (see text). Numbers on curves correspond to chosen values of Q_t/Q_∞ .

behaviour in that they are S-shaped and the uptake data on all membranes are not superimposable when plotted against the reduced parameter $t^{1/2}/l$. Thus in contrast to the patterns described by equation (3), the initial slope of curves 1 and 4 of Figure 2a increases with increasing l . This latter trend, which is typical for all sets of absorption and desorption runs, was also apparent when the published data on Sheppard and Newsome¹ were redrawn. It is directly interpretable by the molecular relaxation model (in any of its three versions), considering that with increasing l the relative importance of relaxation (characterized by the parameter $\alpha = l^2\beta$) decreases in comparison with that of diffusion which is governed by D . With decreasing l the S-shape of the sorption kinetic curves becomes more pronounced (Figure 2a).

On this basis, Kishimoto and Matsumoto¹⁸ obtained D_1 of equation (3) by extrapolating the initial slope l of Q_t/Q_∞ vs. $t^{1/2}/l$ to $l \rightarrow \infty$ for similar sets of sorption curves.

However, since in our data the lack of initial linearity precluded estimation of l to an acceptable degree of accuracy, we have adopted an alternative procedure which enabled us to produce a portion of the hypothetical curve for an infinitely thick membrane (e.g. Figure 2a, curve 5). This was accomplished by plotting $t^{1/2}/l$ vs. $1/l$ for several points on each kinetic curve and extrapolating to zero (e.g. Figure 2b) — a method encouraged by the fact that points for the three thinnest membranes fell on straight lines. From the slope of the resulting, initially linear curve 5 of Figure 2a, D_1 of equation (4) was then obtained. By a comparable extrapolation procedure (i.e. by plotting the same set of data against l) the kinetic curves for $l \rightarrow 0$ (e.g. line 6 of Figure 2a) were obtained, which presumably represent a predominantly relaxation-controlled sorption process (i.e. when $l^2\beta \ll D$).

The integral values $\bar{D}_1(C_0)$ were calculated from the differential diffusion coefficients $\bar{D}_1(C_1, C_0)$ according to the equation:

$$\bar{D}_1(C_0) = \frac{1}{C_0} \int_0^{C_0} D_1(C_0) dC_0 \quad (7)$$

i.e. for a differential sorption step within an interval C_1, C_0 :

$$\bar{D}_1(C_0) = \{C_1 \bar{D}_1(C_1) + (C_0 - C_1) D_1(C_1, C_0)\} / C_0 \quad (8)$$

Figure 3 shows that $\bar{D}_1(C_0)$ obtained in this manner exhibits a positive concentration dependence on the desorption side of the isotherm, while remaining almost constant in absorption. This is in disagreement with the results of Hopfenberg *et al.*¹⁰ who determined the differential values $D_1(C_1, C_0)$ from a similar series of uptake curves (on exactly the same system) by estimating the slopes of the linear portions of the kinetic curves. Their resulting integral coefficients $\bar{D}_1(C_0)$ decreased linearly with increasing concentration on the absorption as well as the desorption side, though the latter values were always higher than the former at any C_0 . Thus, in order to compare the results of these authors with our data we

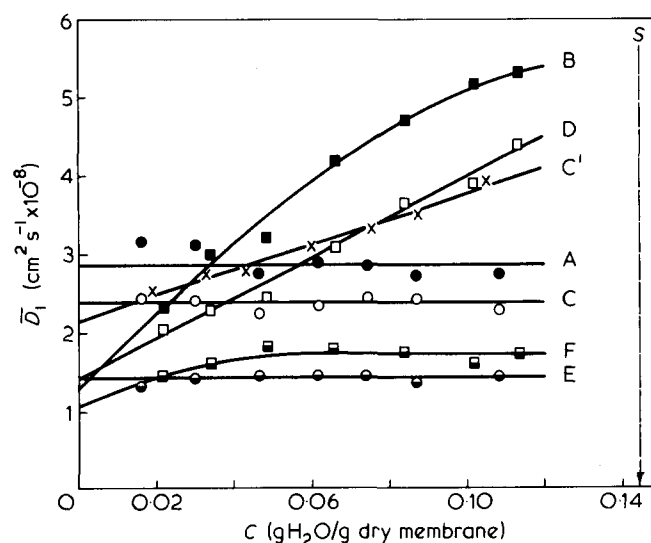


Figure 3 Concentration dependence of \bar{D}_1 from rates of absorption (curves A, C, C', E); desorption (B, D, F). Extrapolation to infinite thickness (A, B). Membranes 3 and 4 of Table 1 (C, C', D and E, F, respectively). Curve C' represents the estimated \bar{D}_m for monomeric species (see text). Dotted line S indicates saturated vapour concentration

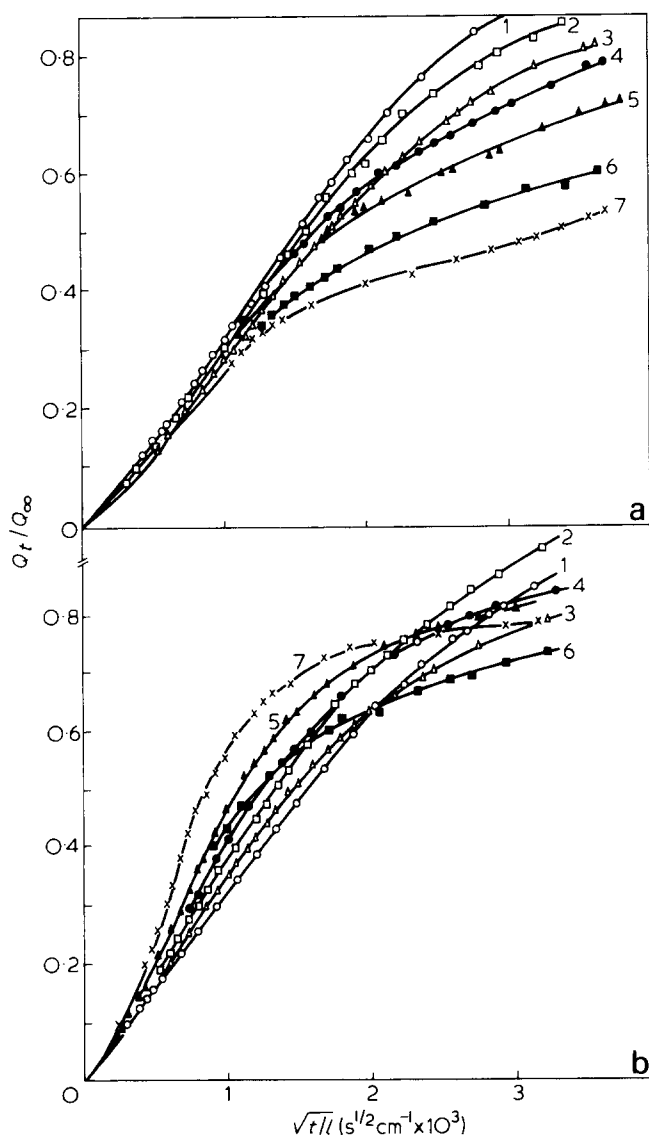


Figure 4 (a) Differential absorption kinetics of membrane 3 of Table 1 with C_0 increasing from 1 to 7 (as labelled) and for the C_0-C_1 intervals shown on curves A and B of Figure 1. (b) Differential desorption kinetics of membrane 3 of Table 1 with C_0 increasing from 1 to 7 (as labelled) and for the C_0-C_1 intervals shown on curve B of Figure 1

have also calculated \bar{D}_1 in the manner described in ref 10 and the resulting concentration dependence for the two extremes in membrane thicknesses is also included in Figure 3 (curves C,D,E,F). These curves give \bar{D}_1 values which are lower than those corresponding to $l \rightarrow \infty$ at any C_0 , but still retain the same general characteristics in the thickest membrane (i.e. \bar{D}_1 increasing with concentration in desorption) whereas for the thinnest membrane \bar{D}_1 tends to become independent of C_0 along both limbs of the isotherm. These trends suggest that for an even thinner membrane the concentration dependence of \bar{D}_1 may appear to reverse (i.e. decrease with increasing C_0) when the slope of the linear portion of a sigmoid sorption kinetic curve is used directly in equation (3). This provides a reasonable explanation for the disagreement between our results and those of Hopfenberg *et al.*¹⁰ who applied this method to membranes with $l \approx 50 \mu\text{m}$, i.e. thinner than any of those used in this study (Table 1). Finally, in order to test our method of extrapolation to infinite thickness on another sort of data, we have made use of the integral absorption kinetic curves of Sheppard and Newsome¹

which yielded a value of $\bar{D}_1 \approx 3.5 \times 10^{-8} \text{ cm}^2 \text{ s}^{-1}$ for $a_0 = 0.9$ on the absorption side, which is comparable to ours; the extrapolation plot corresponding to that in Figure 2b was also linear.

Kinetic plots of $\ln(1 - Q_t/Q_\infty)$ vs. t/l^2 were not linear at any stage up to $Q_t/Q_\infty = 0.97$ and their curvature was more intense in the case of desorption. Similar plots have also been published by Thomas⁶ and by Long and Thompson⁷. This lack of linearity did not allow calculation of D_2 according to equation (4).

DISCUSSION AND CONCLUSIONS

One of the main peculiarities to be interpreted in the data of Figure 3 is the difference in the concentration dependence of the experimental values of \bar{D}_1 between absorption and desorption. A reasonable explanation can be suggested upon careful examination of the family of curves in Figure 4a for absorption on the thickest membrane, in which it is clear that with increasing concentration they tend in some ways to assume a 'two-stage' character¹⁴. In particular, the initial linear portion becomes shorter for each successive concentration increment and at $a_0 \rightarrow 1$ (curves 6, 7) it almost tends to disappear. Thus, for $a_0 > 0.5$ a second stage may be distinguished, whose rate also becomes progressively slower from curves 1 to 7. Similar observations pertain to the absorption kinetic series for all membranes, but not to the corresponding desorption (Figure 4b). This behaviour could be accounted for in terms of the molecular relaxation model if we assume that a relatively fast molecular relaxation during the initial stages of absorption is succeeded by a much slower one¹¹. This could be physically justified by assuming, in turn, that when the available cavities within the polymer structure (which can receive chiefly molecularly-dispersed penetrant with only minor molecular rearrangement) are filled, additional penetrant could still be accommodated, mainly in the form of clusters (probably around the already existing nuclei of monomeric species). The latter process requires the system to undergo more extensive (and hence slower) molecular rearrangement (which may even involve breaking of some interchain bonds) in order to create sufficiently large cavities for penetrant cluster growth. These 'fast' and 'slow' relaxation processes could overlap, so that a true 'two-stage' phenomenon (such as that observed by Newns¹⁹ for the more hydrophilic system, regenerated cellulose-water) is not to be noted in the curves of Figure 4a, with the possible exception of line 7.

The tendency of penetrant molecules to cluster has always been regarded^{11,17,20} as a general characteristic of poor solvents (e.g. water in a relatively hydrophobic polymer) leading to preferential penetrant-penetrant interactions which, under these circumstances, are more favourable energetically than polymer-polymer interactions. Furthermore, at higher activities the tendency to cluster becomes progressively stronger. Consequently, polymer molecular relaxations leading to the formation of cavities capable of accommodating clusters become increasingly favoured thermodynamically at each absorption step. At constant activity such relaxations will lead to higher S , but lower D_1 ^{11,16}. The balance of these opposing tendencies will depend on whether the relaxations in question will also favour increased sorption or mobility of monomeric water. Since clusters of penet-

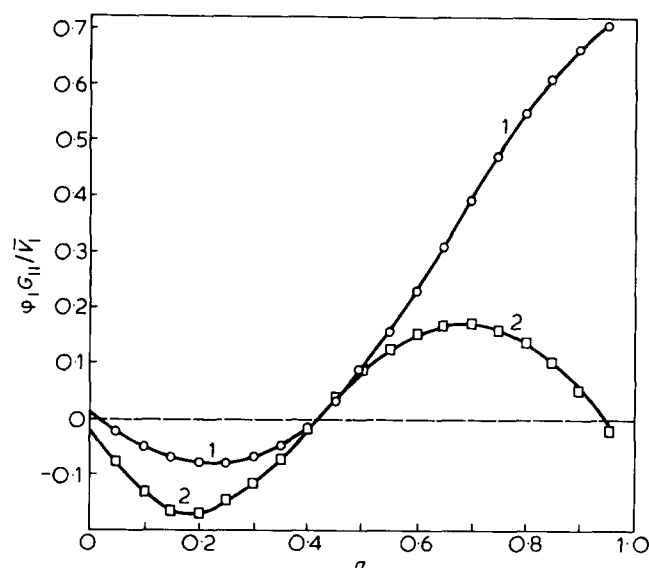


Figure 5 The Zimm-Lundberg cluster function vs. penetrant activity along the absorption and desorption limbs of the hysteresis loop (curves 1 and 2, respectively)

rant may be considered to be essentially immobile, we must have $P_T = SD_T = S_m D_m$, where S_m and D_m refer to monomeric water. Thus, if the net effect of the relaxations is that 'large' cavities (accommodating clusters) grow partly at the expense of 'small' clusters (accommodating monomeric water), we expect P_T to diminish with time (see, example of ethyl cellulose^{11,16,17}). The reverse effect would lead to a P_T increasing with time. This point can be settled only through appropriate permeation measurements to be reported later.

Regardless of the nature of $P_T(a,t)$, the overall description implies that if a hypothetical $Q_\infty(m)$ for the initial absorption stage were known (which would essentially represent the concentration increment ΔC_m of monomeric species), then a significantly higher D_1 (or \bar{D}_1) would be obtained, which would be more appropriate for comparison with those at lower concentrations. Due to the lack of inflection points in most of these two-stage curves (Figure 4a), we have applied an alternative method for obtaining ΔC_m which is identical to that already used by Park²¹ (for estimating pseudo-equilibrium values in the system cellulose acetate-acetone). The long-time experimental curves in Figure 4a were first traced in terms of the short time D_1 in place of D_2 in equation (4) and solving for the appropriate Q_∞ . This lower value of Q_∞ yielded a higher $D_2 = D_m$ which was again used in equation (4) to obtain $Q_\infty(m)$ and hence C_m as well as the concentration of associated water $C_a = C_o - C_m$.

Line C' of Figure 3 shows that \bar{D}_m increases (as predicted) with concentration. On the other hand, lines C and D of Figure 1 indicate that C_m exhibits a Henry law isotherm, while that of C_a (which becomes significant only at $a > 0.5$) is a concave upwards one (type III in Brunauer's classification). Despite the many uncertainties which these calculations entail, we note that a similar 'dual sorption' picture for this system has also been given by Barnes *et al.*²² from equilibrium sorption measurements alone.

Indirect (though more quantitative) support for the above arguments is provided by consideration of the Zimm-Lundberg^{20,23} cluster function G_{11}/\bar{v}_1 within the activity range of our data (Figure 5). This function is related to equilibrium sorption quantities as follows:

$$G_{11}/\bar{v}_1 = -\phi_2 \{ \partial(a/\phi_1) / \partial a \}_{P,T} - 1 \quad (9)$$

where \bar{v}_1 is the partial molar volume of the penetrant and ϕ_1 and ϕ_2 are the volume fractions of the polymer and penetrant, respectively. If $G_{11}/\bar{v}_1 = -1$, the penetrant is randomly dispersed throughout the polymer network, whereas $G_{11}/\bar{v}_1 > -1$ implies that the concentration of sorbate is higher in the neighbourhood of molecules of its own kind (i.e. it tends to form aggregates). Equation (9) was applied to our data by analytical differentiation of our empirical $C=f(a)$ equations for every 0.05 activity increment. These data (Figure 5) suggest that at $a > 0.5$ water molecules seem to increase their association with increasing concentration along the absorption limb of the hysteresis (to a lesser extent this effect is observed along the desorption limb). This trend is in agreement with our conclusions based on kinetic data and it is certainly gratifying that the hypothetical isotherm for C_m (Figure 1) yields $G_{11}/\bar{v}_1 = -1$ whereas that for C_a is responsible for the upward concave behaviour, thus causing the overall G_{11}/\bar{v}_1 to become positive.

An interesting feature of the data in Figure 4b is the pronounced S shape of the desorption vs. $t^{1/2}$ kinetic curves, especially at higher concentrations. We note that Crank's molecular relaxation model¹³, which assumes D alone to be a time-increasing coefficient, leads to S shaped absorption and convex desorption curves. Long and Richman's model¹⁴, however, which considers only C_o to be time variable will produce S shaped desorption vs. $t^{1/2}$ curves when D is not a strongly increasing function of C . Hence, we conclude that both the 'fast' and 'slow' molecular relaxations discerned in our sorption kinetic curves are the result of a time-dependent solubility coefficient. The possibility of non-isothermal diffusion due to the negative heat of absorption²⁴ could not be an exclusive (or even predominant) factor for such small concentration intervals. Furthermore, this effect (prevailing mainly in the early stages of sorption) does not account for the appearance of S shaped curves in both absorption and desorption, considering that its direction in these two cases should have been reversed. Finally, the appearance of S shaped desorption kinetics also precludes interpretation of 'non-Fickian' behaviour in terms of the transverse differential swelling stress model. In this respect we note that according to the proposed versions of this model^{13,25} none of the computed desorption curves should exhibit this feature.

A general conclusion to be drawn is that in view of the long-term molecular relaxations shown to exist, which render the approach to equilibrium extremely slow, our attempted extrapolation to $t \rightarrow \infty$ during the short duration of the early transient state could not be expected to fully separate diffusion from all accompanying rate processes. This analysis was primarily based on the simple model described by equation (6) or the corresponding equation for $D(C,t)$, but a more realistic description¹¹ should contain a spectrum of relaxation frequencies and a concentration dependent β . The same line of reasoning also provides an interpretation for sorption hysteresis, since the time allocated during any normal sorption experiment is insufficient to attain true thermodynamic equilibrium.

ACKNOWLEDGEMENT

This work was sponsored by the Hellenic Atomic Energy Commission. Thanks are due to Dr J. H. Petropoulos for

many fruitful discussions and useful suggestions and to Mr D. Skordilis for laboratory assistance.

REFERENCES

- 1 Sheppard, S. and Newsome, P. *J. Phys. Chem.* 1930, **34**, 1160
- 2 Taylor, R. L., Herman, D. B. and Kemp, A. R. *Ind. Eng. Chem.* 1936, **28**, 1255
- 3 Korverzee, A. E. and Mol, E. A. *J. Polym. Sci.* 1947, **2**, 371
- 4 Hauser, P. M. and McLaren, A. D. *Ind. Eng. Chem.* 1948, **40**, 112
- 5 Kováč, A. *J. Chim. Phys.* 1948, **45**, 258
- 6 Thomas, A. M. *J. Appl. Chem.* 1951, **1**, 141
- 7 Long, F. A. and Thompson, L. J. *J. Polym. Sci.* 1955, **15**, 413
- 8 Korte Falinski, M. *J. Chim. Phys.* 1962, **59**, 27
- 9 Wellons, J. D., Williams, J. L. and Stannett, V. *J. Polym. Sci. (A-1)* 1967, **5**, 1341
- 10 Hopfenberg, H. B., Kimura, F., Rigney, P. T. and Stannett, V. *J. Polym. Sci. (C)* 1969, **28**, 243
- 11 Petropoulos, J. H. and Roussis, P. P. 'Permeability of Plastic Films and Coatings to Gases, Vapours and Liquids' (Ed. H. B. Hopfenberg), Plenum, New York, 1974, pp 21–232
- 12 Crank, J. 'Mathematics of Diffusion', Clarendon, London, 1978, Ch. 4, pp 44–69
- 13 Crank, J. *J. Polym. Sci.* 1953, **11**, 151
- 14 Long, F. A. and Richman, D. *J. Am. Chem. Soc.* 1960, **82**, 513
- 15 Petropoulos, J. H. and Roussis, P. P. *J. Chem. Phys.* 1967, **47**, 1491
- 16 Petropoulos, J. H. and Roussis, P. P. 'Organic Solid State Chemistry' (Ed. G. Adler), Gordon and Breach, London, 1969, Ch 19, pp 343–357
- 17 Petropoulos, J. H. and Roussis, P. P. *J. Polym. Sci. (C)* 1969, **28**, 343
- 18 Kishimoto, A. and Matsumoto, K. *J. Polym. Sci. (A)* 1964, **2**, 679
- 19 News, A. C. *Trans. Faraday Soc.* 1956, **52**, 1533
- 20 Barrie, J. A. 'Diffusion in Polymers' (Eds. J. Crank and G. S. Park), Academic Press, New York, 1968, Ch 8, pp 259–308
- 21 Park, G. S. *Trans. Faraday Soc.* 1961, **57**, 2314
- 22 Barnes, H. M., Skaar, C. and Luner, P. *J. Appl. Polym. Sci.* 1977, **21**, 1085
- 23 Zimm, B. H. and Lundberg, J. L. *J. Phys. Chem.* 1956, **60**, 425
- 24 Armstrong, A. A., Wellons, J. D. and Stannett, V. *Makromol. Chem.* 1966, **95**, 78
- 25 Petropoulos, J. H. and Roussis, P. P. *J. Membrane Sci.* 1978, **3**, 343